Supporting Information

Plimpton et al. 10.1073/pnas.1419595112

SI Materials and Methods

Gβ and PhLP1 Baculovirus Preparation. Human $G\beta_1$ and PhLP1 cDNAs were cloned into the pBlueBac4.5/V5-His-TOPO vector (Invitrogen K2100-20) following the manufacturer's protocol. A C-terminal HPC4 tag (protein C epitope) was added to Gβ, and a C-terminal tobacco etch virus (TEV)-Myc-His_6 tag was added to PhLP1. The Gβ and PhLP1 constructs were cotransfected into Sf9 cells with the Bac-N-Blue vector to facilitate recombination. Successfully recombined baculoviruses were identified by lacZ screening and were isolated by using plaque assays. Clones were amplified in Sf9 cells to produce high-titer baculovirus stocks for expression experiments.

Purification of Gβ-CCT and PhLP1–Gβ-CCT Complexes. High Five cells were grown in EX405 medium and transfected with corresponding Gβ and PhLP1 baculoviruses at an MOI of ∼10. Cells were harvested 72–84 h after transfection, pelleted, and stored at −80 °C. Cells were lysed by two freeze–thaw cycles in liquid nitrogen and a 37 °C water bath (∼10 min) in 3.2 mL of extraction buffer [20 mM Hepes, pH 7.5, 20 mM NaCl, 6 μL/mL protease inhibitor (Sigma P8340), and 0.5 mM PMSF] per gram of cell pellet. Benzonase nuclease was added to a concentration of 24 U/mL, and the lysate was cleared by centrifugation. The extract was layered on a 1 M sucrose cushion in the extraction buffer and centrifuged at 30,000 × *g* for 2 h. An 8-mL fraction was collected from the bottom of the sucrose layer and supplemented with 2 mM $CaCl_2$ and 0.05% CHAPS.

The Gβ-CCT fraction was further purified at 4 °C by using 5 mL of HPC4 antibody resin (Roche 11815024001) equilibrated with equilibration buffer (20 mM Hepes, pH 7.5, 20 mM NaCl, 2 mM $CaCl_2$, and 0.05% CHAPS). The sample was loaded twice and then washed with 35 mL of 20 mM Hepes (pH 7.5), 500 mM NaCl, 2 mM $CaCl_2$, and 7 mL of equilibration buffer. Gβ-CCT complexes were eluted in 20 mM Hepes (pH 7.5), 20 mM NaCl, and 10 mM EDTA. Four elution steps were conducted, each with 5 mL of elution buffer. The first elution included a 30-min release period, and the last three elutions included a 5-min release period. Complexes were concentrated to ∼200 μL by using a 30,000-Da cutoff filter (Sartorius Stedim Biotech VS15RH21), flash-frozen in liquid nitrogen, and stored at −80 °C until cryo-EM analysis was performed.

PhLP1–Gβ-CCT complexes were extracted, lysed, and cleared as described for Gβ-CCT complexes, with the extraction buffer at pH 8.0. CHAPS was added to 0.05%, and the sample was purified at 4 °C by using 3 mL of HisPur cobalt column (Thermo 89964). The column was equilibrated and washed with the extraction buffer supplemented with 0.05% CHAPS. Complexes were loaded and washed three times and then eluted three times with 3 mL of 20 mM Hepes (pH 7.5), 20 mM NaCl, 2 mM $CaCl_2$, 0.05% CHAPS, and 500 mM imidazole. Each elution step included a 10-min release period. The elution product was subsequently purified by using HPC4 antibody resin, concentrated, and stored in the same manner as described for Gβ-CCT complexes.

The composition of the purified Gβ-CCT complex was confirmed by immunoblotting with α-$G\beta_1$ (1), α-CCTα (AbD Serotec MCA2276), α-CCTβ (AbD Serotec MCA2275), and α-CCTζ (MyBioSource MBS6001387). Blots were imaged by using a LI-COR Odyssey infrared scanner. The composition of the purified PhLP1–Gβ-CCT complex was determined by MS. A portion of the purified complex was denatured in urea, alkylated with iodoacetamide, and digested with trypsin. The resulting peptides were analyzed by LC-MS/MS using an LTQ Orbitrap XL instrument. The MS/MS data were analyzed by using the Mascot search engine (2) against the *Drosophila melanogaster* genome database and the human $G\beta_1$ and PhLP1 sequences. The *Drosophila* genome is the closest sequenced genome to that of the High Five cells (*Trichoplusia ni*). The phosphorylation state of purified PhLP1–Gβ-CCT was determined by treating it with alkaline phosphatase and measuring the phosphorylation-dependent mobility shift in 10% SDS/PAGE.

In Vitro PhLP1–Gβγ Assembly. Recombinant $G\gamma_2$-TEV-GST in pETDuet-1 was expressed in *Escherichia coli*, extracted with B-PER reagent (Thermo 78248), and purified on glutathione agarose (Thermo 16100) with a glutathione elution. For the assembly assay, 80 μg of Gγ-TEV-GST was added to 50 μg of phosphorylated PhLP1–Gβ-CCT complex in 500 μL of 20 mM Hepes (pH 7.5), 20 mM NaCl, 10 mM EDTA, 0.2 mM PMSF, and 0.05% CHAPS. The proteins were incubated at 23 °C for 30 min. The mixture was then added to 100 μL of prewashed glutathione agarose and incubated at 4 °C for 30 min. The agarose was washed three times before addition of 100 μL of ProTEV protease solution (Promega V6101) and incubation at 25 °C for 1 h. The TEV cleavage product was obtained by removing the supernatant from the beads. As a negative control, GST was similarly expressed, purified, and incubated with PhLP1-Gβ-CCT complex. Samples were separated by 10% and 16.5% SDS/PAGE and immunoblotted with the following antibodies: α-CCTα (Abcam ab109126), α-PhLP1 (3), α-$G\beta_1$ (1), α-$G\gamma_2$ (Abcam ab57263), and α-GST (Abcam ab92). Blots were imaged by using a LI-COR Odyssey infrared scanner.

Image Processing. For the 3D reconstruction, frozen-hydrated samples were processed without any a priori assumption. First, images were classified into homogenous groups by using reference-free methods [refine2d.py command in EMAN (4) and maximum-likelihood approaches implemented in XMIPP]. Selected averages were used to build a reference volume using common lines. These structures were calculated from images selected by EMAN and were subsequently used for a further refinement by using projection-matching protocols implemented in SPIDER (5). The resolution of the final structures was estimated with the 0.3 criterion for the gold-standard Fourier shell correlation coefficient (FSC) procedure (6). The density map and atomic structures were visualized with UCSF Chimera (7). The threshold was chosen to account for ∼100% of the protein mass. The atomic structure of Gβ from the Gβγ complex (8), the structural model of PhLP1–Gβ complex based on the atomic structure of Pdc–Gβγ (9), and the atomic structure of CCT subunits in its open conformation (10, 11) were manually fitted into the EM density by using Chimera.

UV-Induced Cross-Linking. A pcDNA3 vector containing the aminoacyl–tRNA synthetase for BzF and a pSVBpUC vector containing the amber codon suppressor tRNA were a gift from Thomas Sakmar (Rockefeller University, New York) (12, 13). A pcDNA3.1 B+ vector containing human $G\beta_1$ with a Flag tag at the N terminus was obtained from the Missouri University of Science and Technology cDNA Resource Center. This same vector containing human PhLP1 with a Myc-His tag at the C terminus was prepared previously (14). Gβ and PhLP1 BzF variants were made by substituting TAG for a specific amino acid codon using standard cloning techniques.

HEK-293T cells were cultured in 1:1 DMEM:F-12 medium in 60-mm dishes and transfected at 90% confluency with Lipofectamine 3000 (Invitrogen L3000015) according to the manufacturer's protocol. The relative DNA amounts were 10:1:10 tRNA:aminoacyl-tRNA synthetase:WT or BzF variant of Gβ or PhLP1. For experiments in Fig. 7 *A* and *B*, WT Gβ or PhLP1 was cotransfected at a ratio of 1:5 compared with the BzF variant. Three hours after transfection, cells were fed with medium containing BzF (Bachem F-2800) to a concentration of 1 mM. Cells were harvested 48 h after transfection in 20 mM Hepes (pH 7.5), 150 mM NaCl, 6 μL/mL protease inhibitor (Sigma P8340), 0.6 mM PMSF, and 1% Nonidet P-40. Cleared lysates were exposed to UV light from a 600-W flood lamp (Integrated Dispensing Solutions 100402-600) at a distance of 10 inches and at 4 °C for 2.5 min. Samples were immunoprecipitated with α-Flag (Sigma F3165) or α–c-Myc (Invitrogen 13-2500) antibody, followed by addition of protein A/G agarose (Santa Cruz sc-2003). Samples were separated by 10% SDS/PAGE and immunoblotted with the primary antibodies α-CCTα (Abcam ab109126), α-CCTβ (Abcam ab92746), α-CCTγ (Abcam ab106932), α-CCTδ (Abcam ab129072), α-CCTε (Abcam ab106932), α-CCTζ (Santa Cruz, SC-13897), α-CCTη (Abcam ab170861), and α-CCTθ (AbD Serotec MCA2180), and the secondary antibodies α-mouse (LI-COR 926-32210), α-rat (LI-COR 926-32219), α-goat (LI-COR 926-32214), and α-rabbit (LI-COR 926-32211). Blots were imaged by using a LI-COR Odyssey infrared scanner.

XL-MS. The XL-MS analysis followed the protocol established by Leitner et al. (15). Briefly, 200 μg of purified Gβ-CCT or PhLP1–Gβ-CCT complex was cross-linked in 25 mM Hepes (pH 8.0), 100 mM KCl, and 300 μM 50% mixture of H12/D12 DSS (Creative Molecules 001S) at 37 °C for 30 min. Samples were quenched with 50 mM ammonium bicarbonate at 37 °C for 10 min, dried, and denatured with 8 M urea in 0.1 M Tris·HCl (pH 8.5). Proteins were reduced with 5 mM Tris(2-carboxyethyl)phosphine at 37 °C for 30 min and alkylated with 10 mM iodoacetamide at 25 °C in the dark for 30 min. Urea was diluted to a concentration of 4 M, and proteins were digested with lysyl endopeptidase at 1:50 enzyme-to-substrate ratio at 37 °C for 2 h. Urea was then diluted to a concentration of 1 M, and proteins were digested overnight with trypsin at a 1:50 ratio at 37 °C. Peptides were purified with a C18 cartridge (Waters WAT054955), dried, and resuspended in 25-μL size-exclusion column (SEC) mobile phase (70:30:0.1 water:acetonitrile:TFA). Peptides were separated in SEC mobile phase at a flow rate of 50 μL/min by using a GE AKTApurifier system with a Superdex Peptide PC 3.2/30 column. Enriched cross-link fractions were dried and resuspended in 2% formic acid.

LC-MS/MS was performed on a Thermo Scientific EASY-nLC 1000 Liquid Chromatograph system and Orbitrap Velos Pro mass spectrometer. Peptides were loaded on a 15-cm Picofrit column (New Objective) packed with Reprosil-Pur C18-AQ of 3-μm particle size and 120-Å pore size. Separation was achieved with a gradient of 5–95% acetonitrile in 5% DMSO and 0.1% formic acid over 185 min and at a flow rate of 350 nL/min. MS1 resolution was 30,000 over a scan range of 380–2,000 m/z. Peptides with a charge state 3+ and greater were selected for higher-energy collisional dissociation fragmentation at normalized collision energy (NCE) of 35% with three steps of 10% (stepped NCE) and resolution 7,500. Dynamic exclusion was enabled with a 10-ppm mass window and 1-min time frame. Samples were run in duplicate.

Cross-Linked Peptide Analysis. The xQuest/xProphet pipeline was used to identify cross-linked peptides in the MS datasets (15–17). Tandem mass spectra for parent ions with a mass shift of 12.075321 Da and a charge of 2+ to 7+ were classified as isotopic pairs and evaluated in ion-tag mode with the following parameters: two missed cleavages, 5–50 amino acid peptide length, carbamidomethyl fixed modification (57.02146-Da mass shift), oxidation variable modification (15.99491-Da mass shift), 138.0680796-Da mass shift for intra- and intermolecular cross-links, 156.0786442- and 155.0964278-Da mass shifts for mono-links, MS1 tolerance of 10 ppm, and MS2 tolerance of 0.2 Da for common ions and 0.3 Da for cross-link ions.

Spectra were searched against a protein sequence database containing human $G\beta_1$, human PhLP1 (for the PhLP1–Gβ-CCT complex), and the sequences of *Trichoplusia ni* (High Five cell) CCT subunits α–θ. The *Trichoplusia* sequences were obtained by 5′ and 3′ RACEs of extracted High Five mRNA using the GeneRacer Kit (Invitrogen 45-0168) and degenerate primers targeting CCT. The degenerate primers were designed from alignments of *Spodoptera frugiperda* and *Bombyx mori* CCT sequences. The *Trichoplusia* sequences are available in GenBank. The *S. frugiperda* sequence of a 50-amino-acid region of *Trichoplusia* CCTδ that was not obtained via RACE was included in the *Trichoplusia* CCTδ sequence for the xQuest search database.

Cross-link hits were filtered with the following thresholds: ≤10% false detection rate, ≥10% TIC, −4 to 7 ppm MS1 tolerance window, ≥24 xQuest Id-Score for Gβ-CCT analysis, ≥25 xQuest Id-Score for PhLP1–Gβ-CCT analysis, and ≥4 fragmentation events per peptide. Hits meeting these thresholds were manually inspected for the quality of their spectra as well.

Structural Representations. The human $G\beta_1$ protein sequence (P62873) was modeled on the bovine $G\beta_1$ structure of 2TRC by using SWISS-MODEL (18, 19). The human PhLP1 protein sequence (Q13371) was modeled by using I-TASSER (20, 21). These two protein models were structurally aligned according to the Gβ-Pdc interaction of 2TRC to represent the Gβ-PhLP1 complex. *Trichoplusia* CCTα-θ protein sequences were modeled by using SWISS-MODEL on 2XSM, the open form of CCT, to represent the CCT ring shown binding to Gβ and PhLP1. The structures of Gα and Gγ in Fig. 7*C* are from 1GOT and 2TRC, respectively. Structural representations and distance measurements were performed by using UCSF Chimera (7). Chimera was developed by the Resource for Biocomputing, Visualization, and Informatics at the University of California, San Francisco (supported by National Institute of General Medical Sciences Grant P41-GM103311). Some distance measurements were also performed by using xWalk (22). For XL-MS cross-links involving lysines at CCT termini that lacked structural information, the distance was measured from the nearest residue with structural information.

1. Lee BY, Thulin CD, Willardson BM (2004) Site-specific phosphorylation of phosducin in intact retina. Dynamics of phosphorylation and effects on G protein β γ dimer binding. *J Biol Chem* 279(52):54008–54017.
2. Perkins DN, Pappin DJ, Creasy DM, Cottrell JS (1999) Probability-based protein identification by searching sequence databases using mass spectrometry data. *Electrophoresis* 20(18):3551–3567.
3. Thulin CD, et al. (1999) The immunolocalization and divergent roles of phosducin and phosducin-like protein in the retina. *Mol Vis* 5:40.
4. Ludtke SJ, Baldwin PR, Chiu W (1999) EMAN: Semiautomated software for high-resolution single-particle reconstructions. *J Struct Biol* 128(1):82–97.
5. Frank J, et al. (1996) SPIDER and WEB: Processing and visualization of images in 3D electron microscopy and related fields. *J Struct Biol* 116(1):190–199.
6. Scheres SH (2012) RELION: Implementation of a Bayesian approach to cryo-EM structure determination. *J Struct Biol* 180(3):519–530.
7. Pettersen EF, et al. (2004) UCSF Chimera—a visualization system for exploratory research and analysis. *J Comput Chem* 25(13):1605–1612.
8. Sondek J, Bohm A, Lambright DG, Hamm HE, Sigler PB (1996) Crystal structure of a G-protein beta gamma dimer at 2.1A resolution. *Nature* 379(6563):369–374.
9. Gaudet R, Bohm A, Sigler PB (1996) Crystal structure at 2.4 angstroms resolution of the complex of transducin betagamma and its regulator, phosducin. *Cell* 87(3):577–588.
10. Muñoz IG, et al. (2011) Crystal structure of the open conformation of the mammalian chaperonin CCT in complex with tubulin. *Nat Struct Mol Biol* 18(1):14–19.
11. Kalisman N, Schröder GF, Levitt M (2013) The crystal structures of the eukaryotic chaperonin CCT reveal its functional partitioning. *Structure* 21(4):540–549.

12. Grunbeck A, et al. (2012) Genetically encoded photo-cross-linkers map the binding site of an allosteric drug on a G protein-coupled receptor. *ACS Chem Biol* 7(6): 967–972.
13. Grunbeck A, Huber T, Sakmar TP (2013) Mapping a ligand binding site using genetically encoded photoactivatable crosslinkers. *Methods Enzymol* 520:307–322.
14. Lukov GL, Hu T, McLaughlin JN, Hamm HE, Willardson BM (2005) Phosducin-like protein acts as a molecular chaperone for G protein betagamma dimer assembly. *EMBO J* 24(11):1965–1975.
15. Leitner A, Walzthoeni T, Aebersold R (2014) Lysine-specific chemical cross-linking of protein complexes and identification of cross-linking sites using LC-MS/MS and the xQuest/xProphet software pipeline. *Nat Protoc* 9(1):120–137.
16. Rinner O, et al. (2008) Identification of cross-linked peptides from large sequence databases. *Nat Methods* 5(4):315–318.
17. Walzthoeni T, et al. (2012) False discovery rate estimation for cross-linked peptides identified by mass spectrometry. *Nat Methods* 9(9):901–903.
18. Biasini M, et al. (2014) SWISS-MODEL: Modelling protein tertiary and quaternary structure using evolutionary information. *Nucleic Acids Res* 42(web server issue): W252–258.
19. Kiefer F, Arnold K, Künzli M, Bordoli L, Schwede T (2009) The SWISS-MODEL Repository and associated resources. *Nucleic Acids Res* 37(database issue):D387–D392.
20. Roy A, Kucukural A, Zhang Y (2010) I-TASSER: A unified platform for automated protein structure and function prediction. *Nat Protoc* 5(4):725–738.
21. Zhang Y (2008) I-TASSER server for protein 3D structure prediction. *BMC Bioinformatics* 9:40.
22. Kahraman A, Malmstrom L, Aebersold R (2011) Xwalk: computing and visualizing distances in cross-linking experiments. *Bioinformatics* 27(15):2163–2164.

A

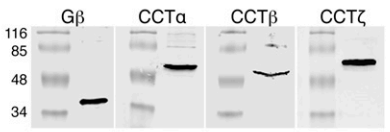

B

Categories	Protein	Sequence (Matched Peptide)
Protein	CCT-alpha	MSTLASPLSI AGTRQSGASV RTQNVMAALS ISNIVKSSLG PVGLDKMLVD DIGDVTVTND GATILKLLEV EHPAAKVLVE LAQLQDEEVG DGTTSVVILA AELLKNADEL VKQKIHPTSI ISGYRIACKE ACKYISEHLT APVDELGRDS LINIAKTSMS SKIIGADAEF FSAMVVDAAQ SVKITDPRGQ AAYSIKAINV LKAHGKSARE SVLIPGYALN CTIASQQMPK KIVNAKIACL DFSLQKTKMK MGVQVLINDP DKLEAIRARE LDITKERINM ILGTGVNMVL VSGGVDDLCM KYFVEAGAMA VRAVKSDLKK IIAKATGAAF ITSLTNMDGE ESFDASMVGE AAEVAQERIC DDELILIKGT KARAAASILL RGPNDFYCDE MERSVHDALC VVKRVLESKK VVAGGGCVEA ALSIYLENFA TSLASREQLA IAEFAKSLLV IPKTLSVNAA KDATDLVAKL RSYHNSSQTK PERSDLKWTG LDLIEGVVRD NKKAGVLEPA MSKIKSLKFA TEAAITILRI DDMIKLNPED KSGKSYADAC AAGELDG
Protein	CCT-beta	MSLNPVRVLK NEAQEEKAEM ARLSSFIGAI ATGDLVKSTL GPKGMDKILV ATGRNAGHVE VTNDGATILK AVGVDNPAAK ILVDMSRVQD EEVGDGTTSV TVLASELLRE AEKLVEQKLH PQIIVSGWRQ ATQVALEALT AAAQDNSSSD EKFRNDLLNI ARTTLSSKIL HQHKDFFANL AVDAVMRLKG SGELKSIQII KKSGGTLGDS FLDEGFLLDK KPGVHQPQRI ENARILIANT PMDTDKIKVF GSSIKVDSLA KIADLEMAEK EKMKEKVDKI LKHKCNVFIN RQLIYNYPEQ LFADAAVMSI EHADFDGIER LAYCTGGEIV STFENPSLVK LGECDVIEQV MIGEDTLLRF SGVKLGEACT IVIRGATQQI LDEADRSLHD AICVLAATVK ESRIIFGGGC SEALMATAVL KKAAETPGKE AIAIEAFARA LLSLPTAIAD NAGYDSAQLV SELRAGHAQG KQTLGLDMEL GKVADVRELG ITESFAVKRQ VLMSASEAAE MILRVDNIIR CAPRRRVPDR GYC
Protein	CCT-gamma	MFGGQQPILV LSQNTKRESG RKVQLENIQA GKAIADVIRT CLGPQAMLKM LMDPMGGIVM TNDGNAILRE ITVQHPAAKS MIEIARTQDE EVGDGTTSVI VLAGEMLAAA EPFLQQQIHP TVIIRAYREA LEDIVGHLQS QLSIQLDVKD KAKMADVVKA CVGTKFIGKW SDLAVKIALD AVETVTLSEN GRLEVDIKRY AKVEKIPGGA IESSCVLKGV MINKDVTHPK MRRLIENPRI VLLDCSLEYK KGESQTNVEI IGEQDFTRML QIEEEFVQRI CADIIAVKPD LVFTEKGVSD LAQHYLLKAG ITAIRRLRKT DNLRIARACG ATIVNRTEEL TEKDVGTGAG LFEVKKIGDE YFTFVTECKE PKACTILLRG ASKDILNETE RNLQDALHVA RNLVLEPRLV AGGGAVEMAA SQLLTRKQVK GPYTAVAHAL EIIPRTLAQN CGANTIRALT ALRAKHASHT GDGVCAWGID GESGEIVDMN VKNIWEPLAV KLQTYKTAVE TAILLLRIDD IVSGSKKRGG NEPTNPAAMA QGQE
Protein	CCT-delta	MAPKAAAVNI KPTAKAFKDE SKFTDVRLSN IQAAKAVSDA IRTSLGPRGM DKMIQAGNGE VSITNDGATI LKQMNVLHPA AKMLVELSKA QDVAAGDGTT SVVVIAGALL EACEKLLQKG LHPTAISDSF QRCSNKAVEI LKQMSTPIEL DDRETLIKSA STSLNSKVVS QQSSLLAPIA VDAVLKVTDP GKETSVDLKN IKVISSLGGT VEDTELVDGL VFTCRSAGSN APKRIEKAKI GLIQFCISAP KTDMDSHVIV SDYAAMDKVL KEERSYILNI VKQIKKSGCN VLLVQKSILR DAVSDLAQHF LDKICMVVK DVEREDIEFV CKTLHCRPIA SLDHFTAENL SSADLVERVA SGTNKFVKIT GIQNMGRTVS IICRGSNKLV LEEAARSLHD ALCVVRCLVK LRAQIVGGGA PEIEMALQLA ALAQTVEGVD AYCFRAFADA LEVIPSTLAE NAGLNPIATV TELRNRHAQG EKNAGINVRK GAITDIFAEN VVQPLLVSIS SITLATETIR SILKIDDIVN TFS
Protein	CCT-epsilon	MPCVQLTHIM AAKQIASTLK TSLGPKGLDK IMVSPDGDVT VTNDGATIMK LMEVDHEIAK LMVQLSQSQD DEIGDGTTGV VVLAGALLEQ AEGLIDRGIH PIRIADGFEL AAQCAIKQLD AIAQPFFPVD KNKEPLIQIA MTTLGSKIVN KCHRQMAEMA VDAVLNVADI EKKDVNFELI KIETKVGGRM EDSMLVKGVI VDKTLSHSQM PKELKNVKLA ILTCPFEPPK PKTKHKLDVT SAEDYRALRE YEQRKFTQMV KQVKDAGATL AICQWGFDDE ANHLLLQQEL PAVRWVGGPE IELIAIATGG RIVPRFEELT PEKLGVAGLV REMAFGTSKD KMLVIEECKN SKAVTIFLRG GNAMIIAEAA RSIHDAICVV RSLVKDSRIV YGGGAAEISC SLAVAKEADQ LSTLEQYAFR AFSVALESIP LALAENSGLH PIETLSELKA RQVAEKKSSL GVDCMLSGDS DMKSHNVVES LHSKKQQILL STQLVKMILK IDDVRSKNEG GM
Protein	CCT-zeta	MASISLLNPK AEFAAAAQAL AINISAAKGL QDVMRTNLGP KGTVKMLVSG AGDIKITKDG NVLLHEMQIQ HPTASMIARA STAQDDSTGD GTTTTVMLIG ELLKQADIYL SEGLHPRIMT DGFEKARDKA LEVLDQVKVP VEINKKNLVE VANTSLKTKV HPALADLLTD VCVNAVLTIA SADKTKPVDL HMVELMEMQH KSDTDTQLVR GLVMDHGARH PDMPKRLENA YILTANVSLE YEKAEVNSGF FYKTAEEREA FVRAEREFID QMVKEVIELK RSVCDGTDKT FVLINQKGID PISLDALAKE GILALRRAKR RNMERLSLAC GGTAMNSFDD LQEEHLGYAG VVYEHVLGEN KYTFVEDCKN PLSVTILIKG PNKHTITQIK DAIRDGLRAI NNTIADKALV PGAGAFEVRA YNELVAFKDT IKGKSRLAVQ AFADALLVIP KTLAVNSGYD AQDTIVKLTV EDRLSPELVG LDLATGEPMK PVDLGVYDNY IVKKQILNSC SIIASNLLLV DEVMRAGMTS LKG
Protein	CCT-eta	MQFQIVLLKE GTDSSQGKFQ LVSNINACQS IVDAVRTTLG PRGMDKLIVD AHGKATISND GATIMKLLEI IHPAAKTLVD IAKSQDAEVG DGTTSVVLLA GEFLKQVKPF VEEGVHPRVI IKAIRKALQL CMEKINEMAV QIVEQSKDQQ RALLEKCAAT AMSSKLIHQQ KDFFSRIVVD AVLSLDELLP LNMIGIKKVT GGSLEESQLV SGVAFKKTFS YAGFEMAPKS YDNCKIALLN IELELKAEKD NAEIRVDNVK KYQKVVDAEW QILYNKLAKI HESGANVVLS KLPIGDVATQ YFADRDIFCA GRVPEEDLKR TMKACGGAVM TTANDIKPNV LGLCEHFEER QVGGERFNLF QGCPNAKTST LILRGGAEQF LEETERSLHD AIMIVRRTIK HDSVVAGGGA IEMELSKLLR DYSRTIAGKE QLLIAAIAKG LEIIPRQLCD NAGFDATNIL NKLRQKHAQG GQWYGVDINK EDISDNYEQC VWEPSIIKIN ALTAAAEAAC MILSVDETIK SPKAGEPPMA GGGMGMGRGM GRPM
Protein	CCT-theta	MALSVPKAFG VSQMLKDGAR MYSGLEEAVF RNISACKEFA QTMRSAYGFN GMNKMIINHI EKQFVTSDAG TIMRELDVEH PAAKLIVMAS QMQDAEVGDG TNFVVVLAGA LLESAEELLR LGIITAEISD GYEKALEKAL EILPNLVSHK IEDYRNVEKV KEVLRTSIMS KQYGQEDFLN DLVSKACVSI LPDEGTFNVD NIRICKILGS GLTKSEVVRG MVFKRFVEGD VTYAEKAKIV IFSCPVDIIQ TETKGTVLIK SADELLSFSS GEEELLESQI KAIADAGVKV VVAGGKVGDM ALHFLNKYGL MAVRLNSKFD LRRLSRSVNA TVLPRITTPS QEELGYCDKV CIEELGDTTI VAFRNEGKDS RIATVVIRGA TDNFMDDIER ALDDAINNFK CLTRDGRYLP GAGATEIELA TQLSAYADTL PGLDQYAVRK FANALEVFPK ALAENSGING TEIVNQLYLA HNNEAGKTIG FDIEAEKAST IDTTKAKLFD LYQSKFWGLK YAVGAAATIL KVDQIIMAKR AGGPKVRQAA GSDDES
Protein	G-beta	MSELDQLRQE AEQLKNQIRD ARKACADATL SQITNNIDPV GRIQMRTRRT LRGHLAKIYA MHWGTDSRLL VSASQDGKLI IWDSYTTNKV HAIPLRSSWV MTCAYAPSGN YVACGGLDNI CSIYNLKTRE GNVRVSRELA GHTGYLSCCR FLDDNQIVTS SGDTTCALWD IETGQQTTTF TGHTGDVMSL SLAPDTRLFV SGACDASAKL WDVREGMCRQ TFTGHESDIN AICFFPNGNA FATGSDDATC RLFDLRADQE LMTYSHDNII CGITSVSFSK SGRLLLAGYD DFNCNVWDAL KADRAGVLAG HDNRVSCLGV TDDGMAVATG SWDSFLKIWN
Protein	PhLP1	MTTLDDKLLG EKLQYYYSSS EDEDSDHEDK DRGRCAPASS SVPAEAELAG EGISVNTGPK GVINDWRFK QLETEQREEQ CREMERLIKK LSMTCRSHLD EEEEQQFQKD LQEKISGKMT LKEFAIMNED QDDEEFLQQY RQRMEEMRQ QLHKGPQFKQ VFEISSGEGF LDMIDWEQKS IVIMVHIYED GIPGTEAMNG CMICLAAEYP AVKFCKVKSS VIGASSQFTR NALPALLIYK GGELIGNFVR VTDQLGDDFF AVDLEAFLQE FGLLPEKEVL VLTSVRNSAT CHSEDSDLEI D

Fig. S1. Characterization of purified Gβ-CCT and PhLP1–Gβ-CCT. (*A*) Immunoblots are shown of the purified Gβ-CCT complex probed with antibodies against $G\beta_1$, CCTα, CCTβ, and CCTζ. (*B*) MS identification of the PhLP1–Gβ-CCT complex. Amino acid sequences in red indicate peptide matches found when the MS/MS data were searched against the *Drosophila* database and the human $G\beta_1$ and PhLP1 sequences using Mascot.

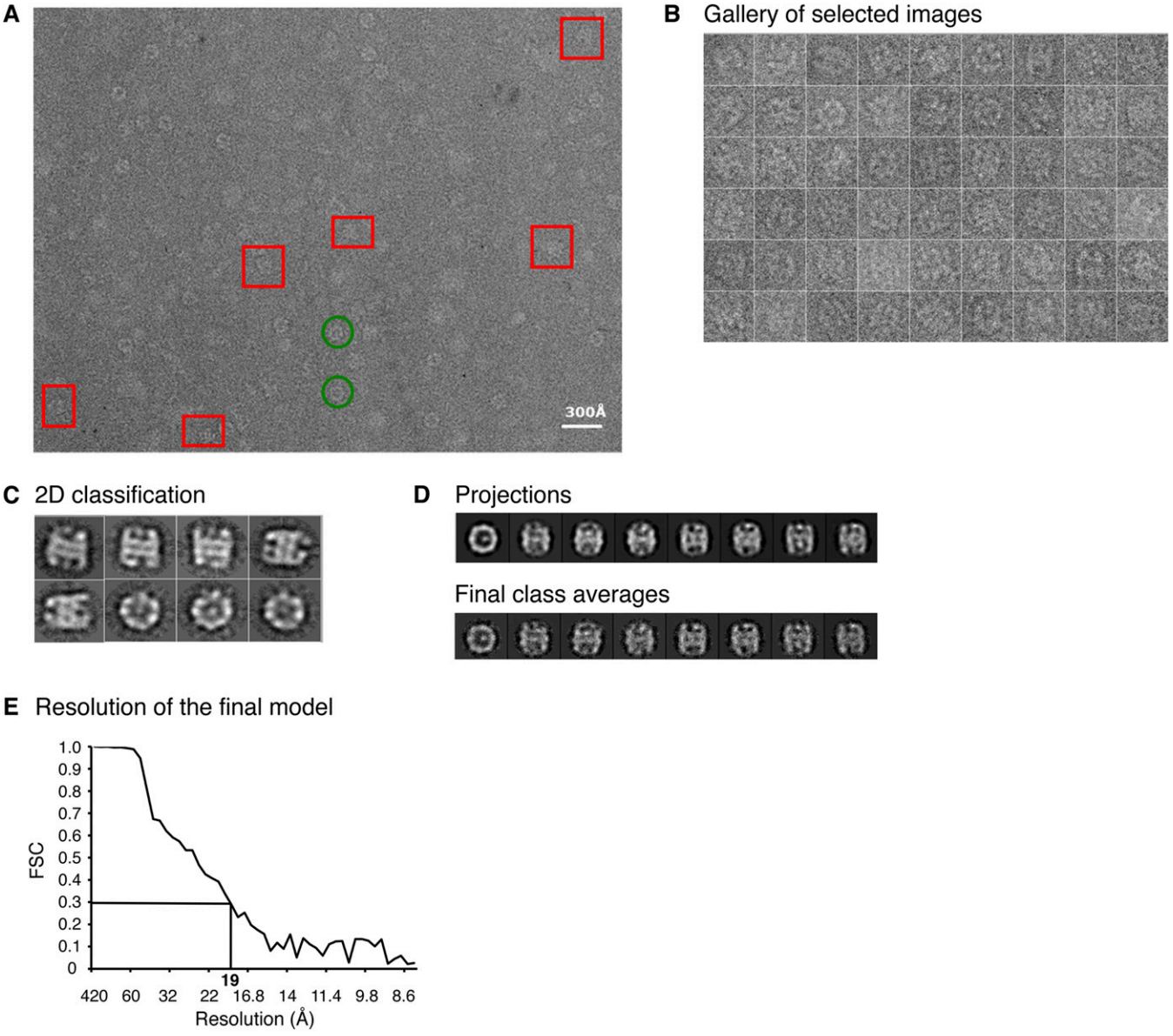

Fig. S2. Gβ-CCT cryo-EM image analysis. (*A*) An EM field of Gβ-CCT particles. Green circles indicate top views, and red rectangles indicate side views. (*B*) A gallery of selected particles. (*C*) Maximum-likelihood classification of the particles. The eight main populations are represented. (*D*) *Upper* represents eight different projections of the final volume, and *Lower* shows the corresponding class averages of these projections. (*E*) Plot of the FSC coefficients vs. resolution between two independent reconstructions for the Gβ-CCT complex using the gold-standard method. The resolution obtained for a signal to noise ratio (SNR) of 0.3 (19 Å) is indicated.

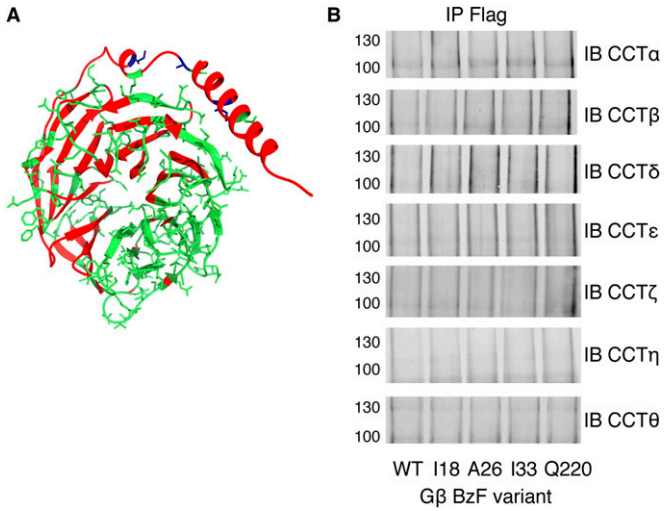

Fig. S3. BzF cross-linking of Gβ. (*A*) Map of BzF insertion positions in Gβ. BzF substitutions were made at the residues shown by green sticks in the Gβ structure. I18, A26, and I33 are shown in blue. A total of 175 substitutions were made. (*B*) Testing for cross-links of the Gβ BzF variants to other CCT subunits. CCT subunit immunoblots are shown of Flag-Gβ immunoprecipitates for the indicated Gβ BzF variants. No cross-linked bands were observed except in the CCTγ blot shown in Fig. 2. WT Gβ and the Q220 BzF variant are included as negative controls.

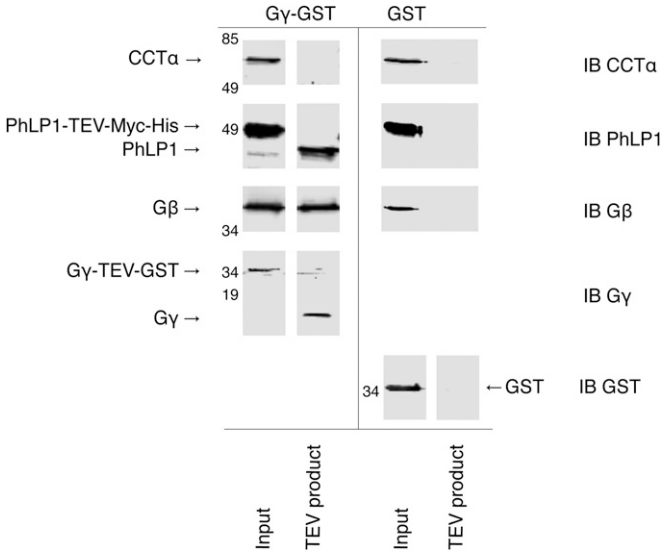

Fig. S4. In vitro assembly of the PhLP1–Gβγ complex. Assessing the ability of Gβ in the PhLP1–Gβ-CCT complex to interact with Gγ in vitro. Purified Gγ–TEV-GST was added to the purified PhLP1–Gβ-CCT complex and incubated to allow Gβγ dimer formation to occur. The Gγ-TEV-GST was precipitated with glutathione beads, and Gγ-containing complexes were released from the beads by cleaving with TEV protease. The TEV supernatant was immunoblotted as indicated. GST without Gγ was tested in parallel as a negative control. The blots show that both PhLP1 and Gβ specifically associated with Gγ, whereas CCTα did not, demonstrating that PhLP1 and Gβ had released from CCT and assembled in a PhLP1–Gβγ complex. Spaces between blots indicate that one gel lane was removed from between the lanes shown without changing the relative mobility or intensity of the blots. The PhLP1 construct also contained a TEV cleavage site, which explains its increased mobility after TEV cleavage.

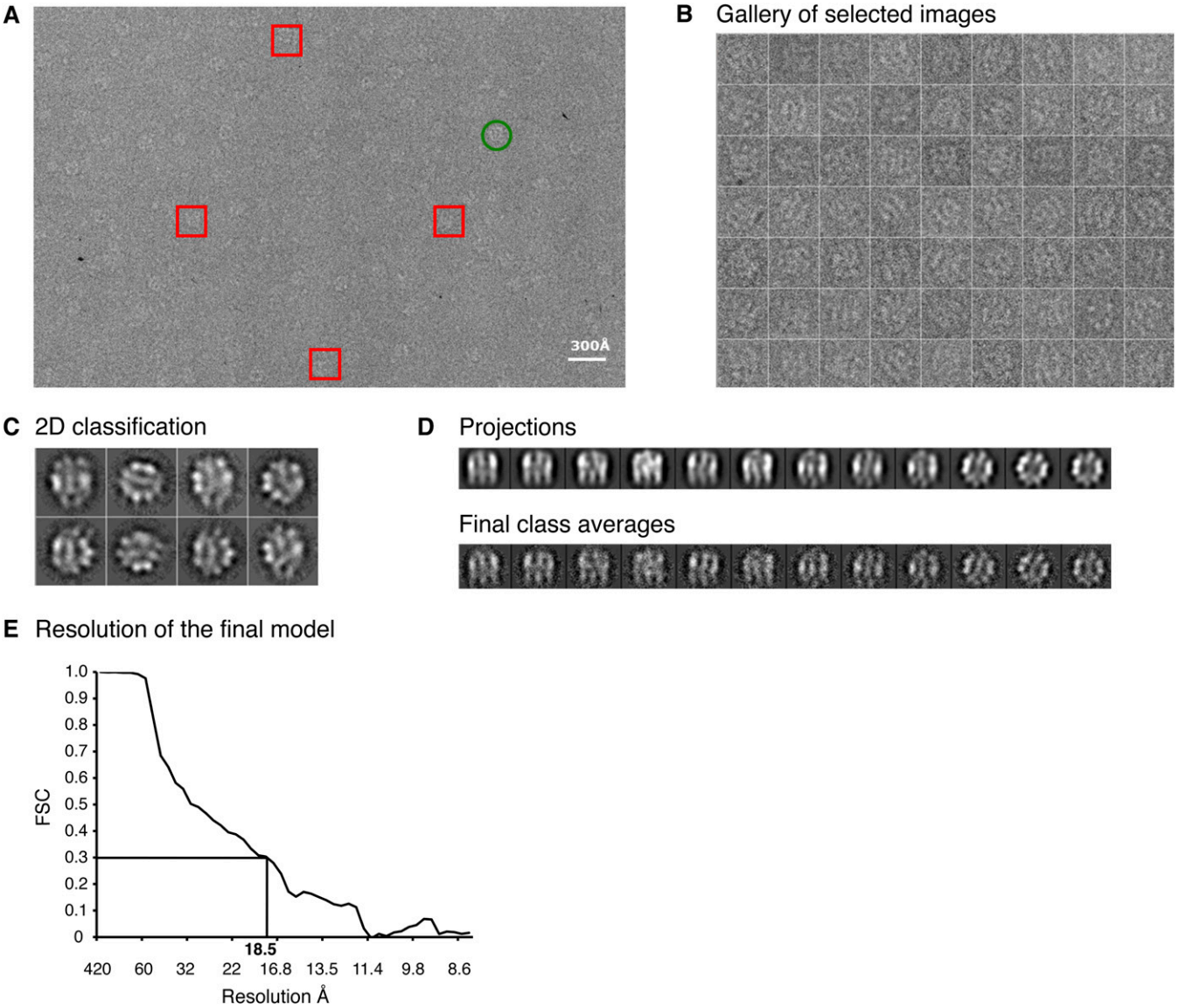

Fig. S5. PhLP1–Gβ-CCT cryo-EM image analysis. (*A*) An EM field of PhLP1–Gβ-CCT particles. The green circle identifies a top view, and red rectangles identify side views. (*B*) A gallery of selected particles. (*C*) Maximum-likelihood classification of the particles. The eight main populations are represented. (*D*) *Upper* represents eight different projections of the final volume, and *Lower* shows the corresponding class averages of these projections. (*E*) Plot of the FSC coefficients vs. resolution between two independent reconstructions for the PhLP1–Gβ-CCT complex using the gold-standard method. The resolution obtained for a SNR of 0.3 (18.5 Å) is indicated.

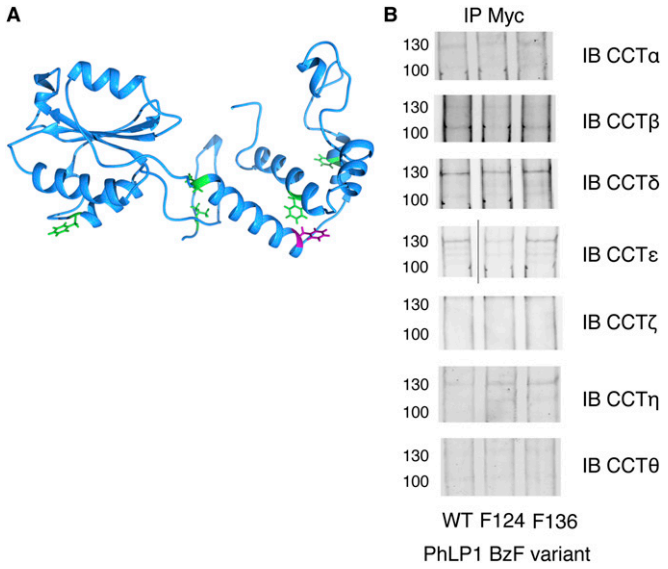

Fig. S6. BzF cross-linking of PhLP1. (*A*) Map of BzF insertion positions in PhLP1. BzF substitutions were made at the residues shown by green sticks in the PhLP1 structure. A total of six substitutions were made. F136 is shown in purple. (*B*) Testing for cross-links of the PhLP1 BzF variants to other CCT subunits. CCT subunit immunoblots are shown of PhLP1-Myc immunoprecipitates for the indicated PhLP1-Myc BzF variants. No unique cross-linked bands, not seen in the WT negative control, were observed for any of the subunits, except for the F136 sample in the CCTγ blot in Fig. 5. The F124 BzF variant is included as an additional negative control. In the CCTε blot, the line indicates that a lane between the WT and F124 sample was removed for clarity of presentation without changing the relative mobility or intensity of the bands.

Dataset S1. XL-MS of the Gβ-CCT complex

Dataset S1

Results of the xQuest/xProphet analysis of cross-linked Gβ-CCT complexes are shown. The dataset includes statistical information for the cross-linked peptides that passed the filtering steps described in *SI Materials and Methods*. Hits are compiled from multiple sets of sample cross-linking, MS/MS, and xQuest analysis. Thus, the false discovery rate (FDR) and identification (Id)-score values correlate for each individual cross-link but are relative only to other cross-links from the same cross-link sample preparation. The MS1 error (in ppm) and total ion count (TIC) were calculated by xQuest. The Cα–Cα distances were measured between cross-linked lysines of the two peptides. The total number of unique cross-links identified was 219, with 42 interprotein and 177 intraprotein cross-links.

Dataset S2. XL-MS of the PhLP1–Gβ-CCT complex

Dataset S2

Results of the xQuest/xProphet analysis of cross-linked PhLP1-Gβ-CCT complexes are shown and compiled as described for Dataset S1. The total number of unique cross-links identified was 166, with 60 interprotein and 106 intraprotein cross-links.